Crystal Structure of $(Et_2Me_2N)_3Cu_4Cl_{11}$: An Antiferromagnetic Chain of Ferromagnetically Coupled Tetramers

Y. Fujii, Z. Wang, and R. D. Willett*

Department of Chemistry, Washington State University, Pullman, Washington 99164

W. Zhang and C. P. Landee

Department of Physics, Clark University, Worchester, Massachusetts 01610

Received January 18, 1995[⊗]

Crystals of the title compound are orthorhombic, space group $Pna2_1$, with $a = 25.155(5)$ Å, $b = 16.080(3)$ Å, $c = 9.027(2)$ Å, and $V = 3651.2(13)$ Å^3 with $Z = 4$ and $\varrho_{calc} = 1.729$ g cm^{-3}. The structure consists of tribridged $Cu_4Cl_{11}^{3-}$ tetrameric units that are linked into infinite chains through the formation of bibridged Cu_2Cl_2 groups. Refinement of 2915 observed reflections ($|F| \geq 3\sigma(F)$) yielded a value of $R = 0.0516$ and $R_w = 0.0600$. Magnetic susceptibility measurements in the range 4−100 K revealed the presence of dominant ferromagnetic coupling at high temperature with the onset of substantially weaker antiferromagnetic coupling at lower temperature. The data are consistent with ferromagnetic coupling within the tetrameric units ($J/k \sim 50$ K). The ground states of these units ($S = 2$) are essentially fully occupied before the antiferromagnetic interactions become significant. These interactions ($J/k \sim -2.6$ K) link the units into an effective $S = 2$ antiferromagnetic chain.

Introduction

Copper(II) halides provide a plethora of structural characteristics. This is due both to the stereochemical flexibility of the Cu(II) ions[1] and to the nonstereospecific nature and bridging capability of the halide ions. The presence of multiple coordination geometries within the same structure,[2] as well as the almost continuous distribution of geometries,[3] belies the relative insensitivity of the coordination potential surface for copper(II) halides. The ability of the halide ions to form μ_2 or μ_3 bridges, the ability of one to three halides to bridge adjacent copper ions, and the existence of both normal and semicoordinate Cu−X bonds provides a nearly infinite, and certainly unpredictable, array of solid state structures. Certain well-defined classes of structures are formed,[4] but other groups of compounds incorporate aspects of several of the structure types in a single material.

Associated with this structural richness is an associated wealth of physical behavior. Much of the interest has focused on spectroscopic properties.[5] The thermal behavior, with respect to thermochromism[6] or with the onset of the dynamic Jahn−Teller effect,[7] has also attracted considerable attention. Our interest has centered on the influence of coordination geometry and bridging characteristics on the solid state magnetic behavior.[7]

In this paper, we report on a novel compound of stoichiometry $A_3Cu_4Cl_{11}$ encountered in our study of the crystal chemistry of the $Et_{4-n}Me_nNX/CuX_2$ system. Structurally, it embodies elements both of the face-sharing chains of distorted octahedra found in several $ACuCl_3$ or CuX_2L systems[9] and of the edge-sharing polyhedra present in many $A_2Cu_2X_6$ dimer chains.[10] The magnetic behavior is such as to yield an $S = 2$ antiferromagnetic chain at low temperatures. Thus, this represents the first realization of a model system to test the Haldane conjecture for spin systems with $S \geq 2$.

Experimental Section

Brown crystals of the title compound were prepared by the recrystallization of $(Et_2Me_2N)CuCl_3$ from CH_3CN solution containing a small excess of $CuCl_2$. The latter was added to prevent the formation of $(Et_2Me_2N)_2CuCl_4$. Samples of Et_2Me_2NCl had been prepared by the reaction of Et_2MeN with MeI, followed by precipitation of AgI upon addition of AgOH and subsequent acidification with HCl. The trichloride was prepared by crystallization from a solution of 1-propanol containing an approximately 1:1 ratio of $CuCl_2$ and Et_2Me_2NCl.

X-ray diffraction data were collected on a Syntex $P2_1$ diffractometer upgraded to Siemens P4 specifications utilizing the XSCANS set of programs.[11] Important details are specified in Table 1. A small crystal of maximum dimension 0.4 mm was found to be orthorhombic, space group *Pnam* or $Pna2_1$, with $a = 25.155(5)$ Å, $b = 16.080(3)$ Å, and $c = 9.027(2)$ Å with $V = 3651.2(13)$ Å^3 to give $\varrho_{calc} = 1.729$ g cm^{-3} for $Z = 4$. The lattice constants were based on the least-squares refinement of 50 high-angle reflections ($25 \leq 2\theta \leq 30°$) obtained with Mo Kα radiation. A total of 3414 reflections (2915 with $|F| \geq 3\sigma(F)$) were

[⊗] Abstract published in *Advance ACS Abstracts,* May 1, 1995.

(1) Reinen, D. *Comments Inorg. Chem.* **1983**, *2*, 227.
(2) Willett, R. D. *Coord. Chem. Rev.* **1991**, *109*, 181.
(3) (a) Willett, R. D.; Halvorson, K.; Patterson, C. *Acta Crystallogr.* **1990**, *B46*, 508. (b) Blanchette, J.; Willett, R. D. *Inorg. Chem.* **1988**, *27*, 843.
(4) (a) Willett, R. D.; Geiser, U. *Croat. Chem. Acta* **1984**, *57*, 737. (b) Willett, R. D.; Place, H.; Middleton, M. *J. Am. Chem. Soc.* **1988**, *110*, 8639. (c) Geiser, U.; Willett, R. D.; Lindbeck, M.; Emerson, K. *J. Am. Chem. Soc.* **1986**, *108*, 1173. (d) Bond, M. R.; Willett, R. D. *Inorg. Chem.* **1989**, *28*, 3267.
(5) (a) Hitchman, M. A.; Cassidy, P. J. *Inorg. Chem.* **1979**, *18*, 1745. (b) Desjardines, S. R.; Penfield, K. W.; Cohen, S. L.; Musselman, R. L.; Solomon, E. I. *J. Am. Chem. Soc.* **1983**, *105*, 4590. (c) McDonald, R. G.; Hitchman, M. A. *Inorg. Chem.* **1986**, *25*, 3273. (d) Riley, M. J.; Hitchman, M. A. *Inorg. Chem.* **1987**, *26*, 3205.
(6) Bloomquist, D. R.; Willett, R. D. *Coord. Chem. Rev.* **1982**, *47*, 125.
(7) (a) Reinen, D.; Atanasov, M. *Chem. Phys.* **1991**, *155*, 157. (b) Reinen, D.; Friebel. *Struct. Bonding* **1979**, *37*, 1.
(8) (a) Willett, R. D. In *Magneto-Structural Correlations in Exchange Coupled Systems*; Willett, R. D., Gatteschi, D., Kahn, O., Eds.; Plenum: New York, 1985, pp 389−420. (b) Willett, R. D.; Grigereit, T.; Halvorson, K.; Scott, B. *Proc. Indiana Acad. Sci.* **1987**, *98*, 147.
(9) Swank, D. D.; Landee, C. P., Willett, R. D. *Phys. Rev. B*, **1979**, *20*, 2154.
(10) Scott, B.; Willett, R. D. *Inorg. Chim. Acta* **1988**, *141*, 193.
(11) XSCANS2, Siemens Analytical X-ray Instruments, Inc., 1993.

0020-1669/95/1334-2870$09.00/0

Table 1. Crystallographic Data

$C_{18}H_{48}Cl_{11}Cu_4N_3$	space group $Pna2_1$ (No. 33)
fw 950.7	$T = 22$ °C
$a = 25.155(5)$ Å	$\lambda = 0.710\,73$ Å
$b = 16.080(3)$ Å	$\varrho_{calc} = 1.729$ g cm^{-3}
$c = 9.027(2)$ Å	$\mu = 3.12$ cm^{-1}
$V = 3651.2(13)$ Å^3	$R(F_o)^a = 0.0506$
$Z = 4$	$R_w(F_o)^b = 0.062$

$^a R = \Sigma||F_o| - |F_c||/\Sigma|F_o|$. $^b R_w = [\Sigma w(|F_o| - |F_c|)^2/\Sigma|F_o|^2]^{1/2}$.

collected out to $2\theta = 45°$ via an ω scan with variable scan speeds between 3 and 30°/min. Semiempirical absorption corrections were made ($\mu = 3.12$ mm^{-1}) based on ψ scan data, with transmission factors ranging from 0.331 to 0.605.

Structure solution and refinement were carried out in a straightforward fashion utilizing the SHELXTL PLUS crystallographic programs on a Micro VAX 3100 workstation.[12] Intensity statistics indicated the choice of a noncentrosymmetric space group, so solution and refinement were carried out in the space group $Pna2_1$. Initial copper and chlorine positions were obtained via the direct methods routine TREF, and nitrogen and carbon positions were located on subsequent electron difference syntheses. Hydrogen atoms were included at calculated positions. Refinement with anisotropic thermal parameters proceeded to a final R value of 0.051 ($R = \Sigma||F_o| - |F_c||/\Sigma|F_o|$) with $R_w = 0.061$ ($R_w = \Sigma w(|F_o| - |F_c|)^2/\Sigma w|F_o|^2$) where $w^{-1} = \sigma^2(F) + 0.0009F^2$, for 326 parameters. The goodness of fit was 1.40, and the maximum residual on the final difference map was 0.6 e/Å^3. Extinction corrections were applied by the relation $F^* = F[1 + 0.002\chi F^2/\sin(2\theta)]^{-1/4}$ with $\chi = 0.00058(5)$. Refinement of a parameter to determine the correct handedness for the coordinate system of this polar space group was indeterminate. Final positional parameters are given in Table 2 with significant Cu−Cl bond distances and angles given in Tables 3 and 4 respectively. Complete listings of all bond distances and angles are included in the supplementary material.

Magnetic data were collected on a PAR vibrating-sample magnetometer over the temperature range 2.0−100 K on a powdered sample weighing 0.1816 g. The applied magnetic field was 5000 Oe.

Structure Description

The structure consists of discrete cations and of copper(II) chloride anionic chains running parallel to the crystallographic *a* axis. Four crystallographically independent Cu(II) ions exist, two with severely tetragonally elongated octahedral coordination geometry (Cu(3) and Cu(4)) and two with distorted square pyramidal geometry (Cu(1) and Cu(2)). This can be seen in Figure 1. The equatorial Cu−Cl bond distances are typically 2.23−2.34 Å. In the square pyramidal coordinated species, the apical Cu−Cl distances are 2.603(3) Å for Cu(2)−Cl(2) and 2.647(3) Å for Cu(1)−Cl(3) while the smaller of the *trans* angles are 157.7 and 158.1°, respectively. Each elongated octahedron contains one shorter semicoordinate Cu···Cl bond (2.8−2.9 Å) and one very long Cu···Cl interaction (≥ 3.2 Å).

Each Cl^- ion is involved in a μ_2 bridge between pairs of Cu(II) ions, resulting in the formation of the anionic chains. The existence of only bridging halide ions is consistent with the lack of hydrogen bonding or strong electrostatic interaction capability of the cations. Within each chain, tetrameric units can be envisioned in which adjacent coordination polyhedra share faces, as seen in Figure 2. The two distorted octahedral polyhedra are in the middle of each unit, and the square pyramidal polyhedra are at the ends. These define tribridged linkages. The chains are then formed by edge sharing of square pyramidal polyhedra between adjacent tetrameric units. In this manner, bibridged linkages are produced. Systematic variations in the lengths of the equatorial Cu−Cl bonds are associated with the nature of the μ_2 linkages. Those involving two equatorial bonds are longer than normal (2.28−2.34 Å), while the ones with one equatorial and one axial or semicoordinate bond tend to be shorter (2.23−2.29 Å).

For interpretation of the magnetic data, examination of possible interchain interactions is also important. Figure 2 shows that adjacent chains pack in a pseudo hexagonal array with the chains separated by the organic cations. Thus no significant exchange pathways link adjacent chains. Figure 2 also demonstrate that the structure is closely related to the ideal hexagonal ABX_3 structures, despite the loss of chloride ions from within the metal−halide chains. The observed *b*:*c* ratio is 1.781, very close to the ideal value of 1.732 for a hexagonal unit cell indexed on an orthorhombic lattice. Since the cations lack hydrogen bonding capabilities, the interaction between the chains and the cations is purely electrostatic. Similar packing is observed in $(Me_4N)CuCl_3$ and in $(EtMe_3N)_4Cu_5Cl_{14}$. In this latter structure, the smaller cation allows for a 4:5 cation:Cu

(12) SHELXTL PLUS, Siemens Analytical X-ray Instruments, Inc., 1990.

Table 2. Atomic Coordinates ($\times 10^4$) and Equivalent Isotropic Displacement Coefficients (Å$^2 \times 10^3$)

	x	y	z	U(eq)^a
Cu(1)	970(1)	7254(1)	2264	38(1)
Cu(2)	2255(1)	7863(1)	1727(2)	38(1)
Cu(3)	−262(1)	7643(1)	2408(2)	40(1)
Cu(4)	−1503(1)	7519(1)	1912(2)	37(1)
Cl(1)	2910(1)	8235(2)	3407(5)	52(1)
Cl(2)	2840(1)	6533(2)	1518(5)	48(1)
Cl(3)	388(1)	8617(2)	2534(5)	53(1)
Cl(4)	284(1)	6916(2)	705(5)	53(1)
Cl(5)	−853(1)	6537(2)	2457(5)	45(1)
Cl(6)	−806(1)	8320(2)	4046(5)	65(1)
Cl(7)	585(1)	6587(2)	4162(5)	67(1)
Cl(8)	1539(1)	7469(2)	300(5)	54(1)
Cl(9)	1687(1)	7606(2)	3676(5)	59(1)
Cl(10)	2635(1)	8578(2)	−107(5)	63(1)
Cl(11)	−977(1)	8074(2)	158(5)	56(1)
N(1)	879(4)	4096(5)	2228(12)	45(3)
N(2)	810(5)	9139(6)	7215(13)	61(4)
C(4)	930(5)	4244(9)	3878(13)	61(5)
C(1)	1187(7)	3365(9)	1857(22)	129(9)
C(7)	812(6)	8250(8)	6897(22)	93(6)
C(6)	−79(5)	4564(8)	2282(22)	89(7)
C(3)	1625(7)	5078(9)	1590(29)	130(9)
C(5)	342(7)	4009(20)	1935(33)	277(24)
C(2)	1117(7)	4755(13)	1322(20)	135(10)
C(8)	358(10)	9571(16)	6448(29)	223(18)
C(10)	−131(7)	9078(15)	7605(33)	194(15)
C(9)	803(11)	9346(14)	8781(26)	246(24)
N(3)	2351(4)	1080(6)	1779(13)	49(3)
C(11)	2378(7)	924(10)	161(18)	88(7)
C(14)	1617(6)	83(12)	2218(25)	124(9)
C(12)	2794(8)	852(24)	2395(29)	286(26)
C(13)	2308(10)	1900(10)	2033(29)	204(16)
C(18)	3340(5)	695(11)	2084(27)	115(9)
C(16)	1784(6)	9293(11)	6623(29)	124(9)
C(17)	1954(13)	638(22)	2329(29)	428(34)
C(15)	1256(8)	9494(18)	6468(47)	244(23)

^{a} Equivalent isotropic U defined as one-third of the trace of the orthogonalized U_{ij} tensor.

Table 3. Bond Lengths (Å)

Cu(1)−Cu(3)	3.162(2)	Cu(1)−Cl(3)	2.647(3)
Cu(1)−Cl(4)	2.291(4)	Cu(1)−Cl(7)	2.240(4)
Cu(1)−Cl(8)	2.305(4)	Cu(1)−Cl(9)	2.281(3)
Cu(2)−Cl(1)	2.319(4)	Cu(2)−Cl(2)	2.603(3)
Cu(2)−Cl(8)	2.304(3)	Cu(2)−Cl(9)	2.304(4)
Cu(2)−Cl(10)	2.231(4)	Cu(2)−Cu(4a)	3.189(2)
Cu(3)−Cu(4)	3.160(2)	Cu(3)−Cl(3)	2.266(3)
Cu(3)−Cl(4)	2.370(4)	Cu(3)−Cl(5)	2.320(3)
Cu(3)−Cl(6)	2.290(4)	Cu(3)−Cl(11)	2.801(4)
Cu(4)−Cl(5)	2.325(3)	Cu(4)−Cl(6)	2.905(4)
Cu(4)−Cl(11)	2.247(4)	Cl(1)−Cu(4a)	2.339(4)
Cl(2)−Cu(4a)	2.277(3)		

Table 4. Bond Angles (deg)

Cl(3)−Cu(1)−Cl(4)	80.6(1)	Cu(3)−Cu(1)−Cl(7)	68.9(1)
Cl(3)−Cu(1)−Cl(7)	95.0(1)	Cl(4)−Cu(1)−Cl(7)	91.8(1)
Cl(3)−Cu(1)−Cl(8)	106.9(1)	Cl(4)−Cu(1)−Cl(8)	91.7(1)
Cl(7)−Cu(1)−Cl(8)	158.1(1)	Cl(3)−Cu(1)−Cl(9)	100.4(1)
Cl(4)−Cu(1)−Cl(9)	176.1(1)	Cl(7)−Cu(1)−Cl(9)	91.9(1)
Cl(8)−Cu(1)−Cl(9)	84.3(1)	Cl(1)−Cu(2)−Cl(2)	81.8(1)
Cl(1)−Cu(2)−Cl(8)	173.1(2)	Cl(2)−Cu(2)−Cl(8)	100.1(1)
Cl(1)−Cu(2)−Cl(9)	89.3(1)	Cl(2)−Cu(2)−Cl(9)	105.0(1)
Cl(8)−Cu(2)−Cl(9)	83.8(1)	Cl(1)−Cu(2)−Cl(10)	92.7(1)
Cl(2)−Cu(2)−Cl(10)	97.3(1)	Cl(8)−Cu(2)−Cl(10)	93.6(1)
Cl(9)−Cu(2)−Cl(10)	157.7(1)	Cl(3)−Cu(3)−Cl(4)	87.5(1)
Cl(3)−Cu(3)−Cl(5)	172.5(1)	Cl(4)−Cu(3)−Cl(5)	90.3(1)
Cl(3)−Cu(3)−Cl(6)	94.1(1)	Cl(4)−Cu(3)−Cl(6)	178.5(1)
Cl(5)−Cu(3)−Cl(6)	88.2(1)	Cl(3)−Cu(3)−Cl(11)	109.2(1)
Cl(4)−Cu(3)−Cl(11)	91.3(1)	Cl(5)−Cu(3)−Cl(11)	77.9(1)
Cl(6)−Cu(3)−Cl(11)	88.1(1)	Cl(5)−Cu(4)−Cl(6)	74.7(1)
Cu(3)−Cu(4)−Cl(11)	59.6(1)	Cl(5)−Cu(4)−Cl(11)	90.3(1)
Cl(6)−Cu(4)−Cl(11)	86.3(1)	Cl(5)−Cu(4)−Cl(1A)	88.2(1)
Cl(6)−Cu(4)−Cl(1A)	103.2(1)	Cl(11)−Cu(4)−Cl(1A)	169.6(2)
Cl(5)−Cu(4)−Cl(2A)	176.5(2)	Cl(6)−Cu(4)−Cl(2A)	104.2(1)
Cl(11)−Cu(4)−Cl(2A)	92.9(1)	Cl(1A)−Cu(4)−Cl(2A)	88.8(1)
Cu(2)−Cl(1)−Cu(4A)	86.4(1)	Cu(2)−Cl(2)−Cu(4A)	81.3(1)
Cu(1)−Cl(3)−Cu(3)	79.7(1)	Cu(1)−Cl(4)−Cu(3)	85.4(1)
Cu(3)−Cl(5)−Cu(4)	85.7(1)	Cu(3)−Cl(6)−Cu(4)	73.9(1)
Cu(1)−Cl(8)−Cu(2)	95.6(2)	Cu(1)−Cl(9)−Cu(2)	96.2(2)
Cu(3)−Cl(11)−Cu(4)	76.6(1)		

ratio instead of the 3:4 ratio found in the title compound or the 1:1 ratio for the still smaller Me_4N^+ cations.

All three crystallographically independent cations show pronounced librational motion about one of the N−CH_3 bonds. Thermal ellipsoid plots illustrating this phenomenon are included with the supplementary material.

Magnetic Behavior

The plot of $\chi_M T$ vs T shown in Figure 3 leads to a basic understanding of the magnetic behavior. As will be discussed in the following portion of this section, this understanding is consistent with the intuitive expectations based on previously deduced magneto−structural correlations. Specifically, we expect no observable exchange coupling between chains down to 2 K. Also, it is observed that tribridged systems invariably lead to ferromagnetic coupling,[13] while the bibridged linkage can lead to either ferromagnetic or antiferromagnetic coupling depending upon the geometry of the Cu_2X_2 linkage.[14]

In the temperature range 40−100 K, the value of $\chi_M T$ gradually increases as the temperature is lowered. This is indicative of dominant ferromagnetic coupling within the species. In the $1/\chi_M$ vs T plots, the data in the 70−100 K region extrapolate to a Curie−Weiss constant of $\Theta \sim 15$ K, with a Curie constant of approximately 1.66. This is a lower limit for Θ, since some curvature of the plot still exists. The Curie constant corresponds to an average g value of ~2.12 per Cu atom. This value is somewhat too small, indicating that we have not truly reached the high-temperature Curie−Weiss limit. As indicated previously, we associate this ferromagnetic coupling with the tribridged (face sharing) tetrameric unit, leading to an $S = 2$ ground state.

Below 40 K, the product of $\chi_M T$ begins to drop rapidly. This antiferromagnetic coupling is associated with the bibridged linkage. The $1/\chi_M$ vs T plot becomes linear at low temperature and yields a Curie constant of 3.6 and a Curie−Weiss Θ of ~−10 K. The Curie constant is consistent with a spin 2 system with $g \sim 2.18$.

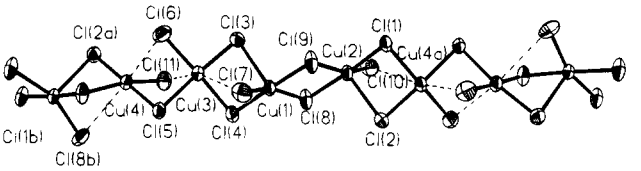

Figure 1. Illustration of the $(Cu_4Cl_{11}^{3-})_n$ chain.

We can model the chain magnetically with a Heisenberg Hamiltonian according to the scheme in **I**. This clearly yields

$$\text{--Cu}(J_1)\text{Cu}(J_2)\text{Cu}(J_3)\text{Cu}(J')\text{---Cu}(J_1)\text{Cu}(J_2)\text{Cu}(J_3)\text{Cu}(J')\text{--}$$

I

too many parameters to extract from powder susceptibility data, so it is necessary to make several simplifying assumptions. It is reasonable to assume that all g values are approximately equal, which should be nearly as good as the assumption of a Heisenberg interaction. From the structural properties, we can suppose that $J_1 \approx J_3$ since the geometries of the interacting copper centers are nearly identical, as is the bridging structure. In the face-sharing arrangements, the dominant exchange pathway in the face sharing is the symmetrical Cu−Cl−Cu linkage. The strength of these interactions will depend upon the Cu−Cl−Cu bond angle and, to a lesser degree, upon the distortion of the primary $CuCl_4$ coordination unit from planarity. The bridging angles are nearly identical for all three exchange pathways (85.5 ± 0.5°). The difference in geometries will lead to differences in the values of the exchange coupling. Nevertheless, we are forced to make a further, most likely reasonable, assumption that all three intratetramer coupling constants are equal; $J_1 \approx J_2 \approx J_3 = J$.

We can further estimate the ratio of J/J' from the ratio of the high and low temperature Curie−Weiss constants, since $\Theta \approx zJS^2$, where z is the number of nearest neighbors. This yields $J/J' \approx 24$. It is thus seen that $J' << J$, so that the intertetramer coupling can be treated in the mean field sense. The model used to analyze the susceptibility data can thus be given by the mean field corrected expression for the susceptibility of a Heisenberg tetramer.[15] This is defined by

$$H = -2J(S_1 \cdot S_2 + S_2 \cdot S_3 + S_3 \cdot S_4)$$

with

$$\chi_M = \chi_{\text{tetramer}} T/(T - \Theta)$$

This fit is very sensitive to the correlation between g and J. With g fixed at a value of 2.18, then $J/k = 50$ K and $\Theta/k = -10.5$ K. With $\Theta = S(S+1)J'z/3k$, we have $J'/k \sim -2.6$ K.

Discussion

The compound reported in this paper is the second member of a new family of compounds with stoichiometry $A_{n-1}Cu_nCl_{3n-1}$. The initial compound reported was $(Me_3EtN)_4Cu_5Cl_{14}$.[16] These contain oligomers of n face-shared polyhedra. The terminal polyhedra are distorted square pyramids while the interior polyhedra are distorted (elongated) octahedra. These oligomers are linked into chains by edge sharing of terminal polyhedra. This family is apparently stable for a fairly narrow range of size for the A cation, in that it appears to be observed for the

(13) Willett, R. D.; Landee, C. P. *J. Appl. Phys.* **1981**, *52*, 2004.
(14) (a) Scott, B.; Willett, R. D. *Inorg. Chim. Acta* **1988**, *141*, 193. (b) Willett, R. D. *Inorg. Chem.* **1986**, *25*, 1918.
(15) Rubenacker, G. V.; Drumheller, J. E.; Emerson, K.; Willett, R. D. *J. Magn. Magn. Mater.* **1986**, *54−57*, 1483.
(16) Bond, M. R.; Willett, R. D.; Rubenaker, G. V. *Inorg. Chem.* **1990**, *29*, 2713.

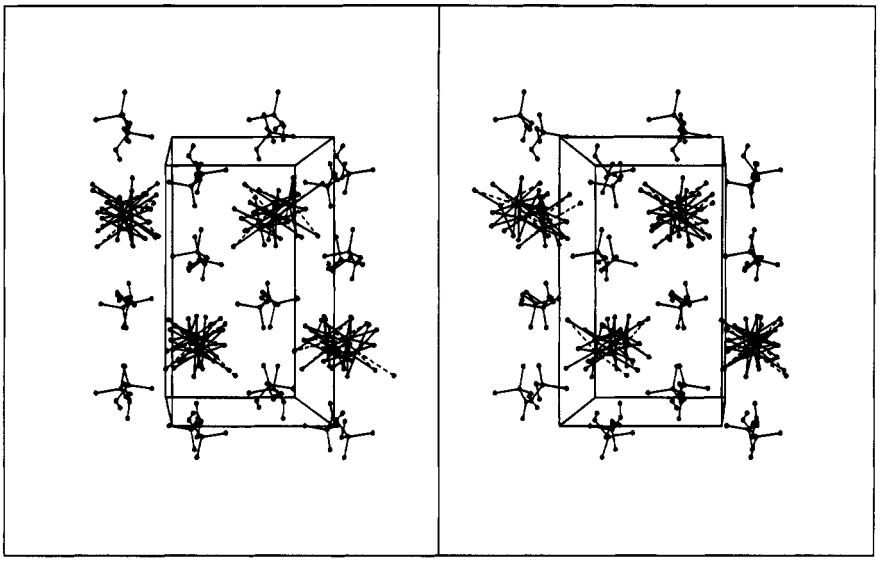

Figure 2. Stereographic packing diagram of the unit cell viewed parallel to the *a* axis.

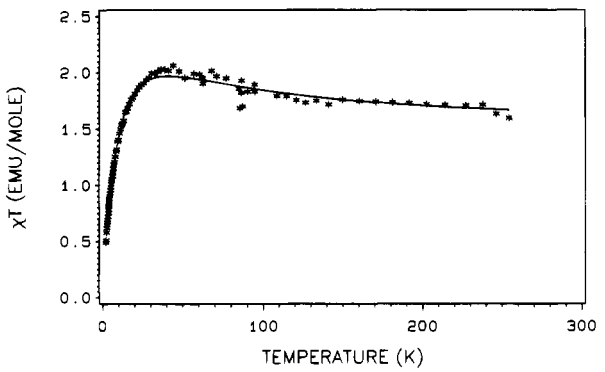

Figure 3. Plot of $\chi_M T$ vs T. Solid curve is calculated with $J/k = 50$ K, $\theta = -10.5$ K, and $g = 2.00$.

Me_3EtN^+ and $Me_2Et_2N^+$ cations only. For A = Me_4N^+, a simple face-shared chain of octahedra is obtained.[17] For larger cations, isolated oligomers are obtained with stoichiometry $A_nCu_nCl_{3n}$ with $n = 2$, 3, or 4.[18] Indeed, even for the $Me_2Et_2N^+$ cation, an isolated $Cu_4Cl_{12}^{4-}$ cation can be obtained.[19]

This family is closely related to a recently reported family of $A_{n-1}Ni_nCl_{3n-1}L_2$ salts with $n = 3$ and 5.[20] These also contain oligomers of n face-shared polyhedra, with the bibridged linkages connecting the oligomers into chains. However, in this case, the additional ligands coordinate to the two terminal Ni atoms of each oligomer, so that all polyhedra have octahedral coordination.

Magnetically, this is a member of a series of copper(II) halide oligomeric chains in which strong ferromagnetic coupling occurs within the oligomer and weaker exhange coupling exists between oligomers. At low temperature, the systems can be approximated as $S = n/2$ chains. Because of the nearly isotropic nature of the exchange coupling in copper(II) salts, these will be realizations of one-dimensional Heisenberg $S = n/2$ systems. Previous examples include $n = 2$ ($S = 1$) chains with both ferro- and antiferromagnetic coupling between oligomers,[21] $n = 3$ ($S = {}^1/_2$) chains with ferromagnetic coupling,[22] and $n = 5$ ($S = {}^5/_2$) chains with antiferromagnetic coupling.[16] This report provides the $S = 2$ antiferromagnetic chain member of the series.

It has not escaped our attention that the title compound may prove useful in an examination of the Haldane gap problem. Haldane[23] predicted that the low-temperature magnetic behavior of one-dimensional Heisenberg antiferromagnets is fundamentally different for integer and half-integer values of the spin. Half-integer values such as $S = {}^1/_2$ have no energy gap between the ground state and the excited states; such systems retain an effective moment as the temperature is reduced to zero. On the other hand, for integer values, the ground state was predicted to be a singlet, separated from the first triplet excited state by an energy gap (the Haldane gap, Δ_H). As the temperature is reduced to zero, the effective moment of integer spin systems was predicted to vanish.

The existence of the Haldane gap, initially highly controversial, has now been well confirmed both theoretically[24] and experimentally for $S = 1$ systems based on chains containing Ni^{2+} ions. However, whether or not the Haldane gap exists for antiferromagnetic Heisenberg chains of $S = 2$ (or higher) spins remains an open question. The major obstacle preventing an experimental test is the absence of appropriate model systems. Ground states with $S = 2$ are found for high-spin Cr^{2+} and Fe^{2+} ions (d^4 and d^6, respectively) in cubic crystal fields. However, the large anisotropies present in these ions make the Heisenberg

(17) Willett, R. D.; Bond, M. R.; Haije, W. G.; Sooniens, O. P. M.; Maaskant, W. J. A. *Inorg. Chem.* **1988**, *27*, 614.
(18) (a) Willett, R. D.; Geiser, U. *Inorg. Chem.* **1986**, *25*, 4558. (b) Scott, B.; Willett, R. D. *J. Am. Chem. Soc.* **1991**, *113*, 5253.
(19) Willett, R. Unpublished (cited in ref 2).
(20) Bond, M. R.; Willett, R. D. *Acta Crystallogr.*, in press.
(21) Scott, B.; Willett, R. D. *J. Appl. Phys.* **1987**, *61*, 3289.
(22) Bond, M. R.; Place, H.; Wang, Z.; Willett, R. D.; Yiu, Y.; Grigereit, T. E.; Drumheller, J. E.; Tuthill, G. F. *Inorg. Chem.* to be submitted for publication.
(23) (a) Haldane, F. D. M. *Phys. Lett.* **1983**, *93A*, 464. (b) *Phys. Rev. Lett.* **1983**, *50*, 1153.
(24) (a) Botet, R.; Jullien, J. *Phys. Rev. B* **1983**, *27*, 613. (b) Botet, R.; Jullien, J.; Kolb, M. *Phys. Rev. B* **1983**, *28*, 3914. (c) Parkinson, J. B.; Bonner, J. C. *Phys. Rev. B.* **1986**, *32*, 4703. (d) Afflec, I. *Phys. Rev. Lett.* **1989**, *62*, 474.
(25) Nightingale, M. P.; Blöte, H. W. J. *Phys. Rev. B* **1986**, *33*, 659.
(26) (a) Renard, J. P.; Verdaguer, M.; Regnault, L. P.; Erkelens, W. A. C.; Rossat-Mignod, J.; Stirling, W. G. *Europhys. Lett.* **1987**, *3*, 945. (b) Ferré, J.; Jamet, J. P.; Landee, C. P.; Reza, K. A.; Renard, J. P. *J. Phys., Colloq.* **1988**, *49*, C8−1441. (c) Ma., S.; Broholm, C.; Reich, D. H.; Stenlieb, B. J.; Erwin, R. W. *Phys. Rev. Lett.* **1992**, *69*, 3571.
(27) (a) Renard, J. P.; Verdaguer, M.; Regnault, L. P.; Erkelens, W. A. C.; Rossat-Mignod, J.; Ribas, J.; Stirling, W. G.; Vettier, C. *Appl. Phys.* **1988**, *63*, 3538. (b) Takeuchi, T.; Ono, M.; Hori, H.; Yosida, T.; Yamagishi, A.; Date, M. *J. Phys. Soc. Jpn.* **1992**, *61*, 3255.
(28) Renard, J. P.; Regnault, L. P.; Verdaguer, M. *J. Phys., Colloq.* **1988**, *49*, C8−1425.
(29) Gadet, V.; Verdaguer, M.; Briois, V.; Gleizes, A.; Renard, J. P.; Beauvillain, P.; Chappert, C.; Goto, T.; Le Dang, K.; Veillet, P. *Phys. Rev. B* **1991**, *44*, 705.

model inappropriate. For these reasons, there have been no experimental tests of $S = 2$ Haldane chains.

The present compound has the potential to test the Haldane conjecture for the case of $S = 2$. As described above, the ferromagnetic coupling within the tetrameric units and the weak antiferromagnetic coupling between the tetramers connects the oligomer into an effective $S = 2$ antiferromagnetic linear chain at low temperatures. Investigation of the magnetic susceptibility and field-dependent magnetization at low temperatures is in progress.

Acknowledgment. This research was supported by NSF Grants DMR-8803382 and DMR-9006470.

Supplementary Material Available: Tables of X-ray data collection parameters, complete bond distances and angles, hydrogen atom positions, and anisotropic thermal parameters and thermal ellipsoid plots of the cations (12 pages).

IC950043U